Preprints of the 21st IFAC World Congress (Virtual)
Berlin, Germany, July 12-17, 2020

Lyapunov Based Hierarchical Trajectory Control of an Autonomous Ground Vehicle Subjected to Slip

Omkar Sudhir Patil * **Shubhendu Bhasin** **

* *Department of Mechanical and Aerospace Engineering, University of Florida, Gainesville FL 32611-6250 USA. (email : patilomkarsudhir@ufl.edu)*
** *Department of Electrical Engineering, Indian Institute of Technology Delhi, New Delhi-110016, India. (email : sbhasin@ee.iitd.ac.in)*

Abstract: The dynamics of wheel slip plays an important role in generation of traction forces, responsible for driving a ground vehicle. It is important to take these dynamics into account while designing control laws, in order to ensure stability of the autonomous vehicle. In this paper, the longitudinal and lateral slip dynamics are modeled and incorporated in the vehicle model. The key contribution of this paper is the design of a nonlinear hierarchical controller to address the trajectory tracking problem in presence of combined longitudinal and lateral slip dynamics. A Lyapunov based analysis is used to guarantee stability of the closed-loop system. Simulation results are provided to demonstrate the efficacy of the proposed controller.

1. INTRODUCTION

The study of autonomous ground vehicles has attracted significant attention in recent years. Particularly, control design is an important aspect of research related to both, autonomous ground vehicles as well as wheeled mobile robot platforms. Typical problems in this context are trajectory tracking and path tracking. The trajectory tracking problem involves design of control laws such that a time parameterized reference (i.e., a planned geometric path with associated timing law) is tracked, while the path tracking problem requires the vehicle to converge to and follow a path without any timing law (Aguiar and Hespanha (2007)).

Often, the longitudinal (cruise control) and lateral control (automated lane-keeping) aspects of path or trajectory tracking problem are separately discussed (Rajamani (2011)), where only the longitudinal slip dynamics is considered for longitudinal control and only the lateral slip dynamics for lateral control. The lateral controller is designed under the constant longitudinal velocity assumption, for which a linearized model of vehicle is obtained. Similarly, a nonlinear lateral controller is designed in Jiang and Astolfi (2018), with the assumption of constant longitudinal velocity. However, this assumption may not be reasonable for the path tracking or the trajectory tracking problem, particularly when longitudinal slip is also present. Without the assumption of a constant longitudinal velocity, the nonlinear coupling between the longitudinal and lateral vehicle dynamics complicates the design of a stabilising controller.

A hierarchical adaptive controller for path tracking problem involving autonomous vehicles is adopted in (Chen et al. (2015)), which involves decoupling of high-level dynamics vehicle motion from the low-level dynamics of slip. Although there has been considerable research on the path tracking/lane following problem involving autonomous vehicles, few results exist that address the trajectory tracking problem. Unfortunately, the control design for the path tracking problem does not trivially extend to the trajectory tracking case, since the trajectory tracking problem additionally requires to follow a timing law (Aguiar and Hespanha (2007)).

A non-linear model predictive controller is proposed for controlling an autonomous vehicle in (Falcone et al. (2007); Quirynen et al. (2018)), considering longitudinal as well as lateral slip dynamics. While there is a significant amount of literature involving MPC based techniques to solve the trajectory tracking problem in presence of combined longitudinal and lateral slip, there is almost no attempt to solve this problem in the framework of Lyapunov based stability analysis, to the best of the authors' knowledge.

Introducing the slip dynamics yields a unique coupled structure of combined vehicle dynamics, which causes difficulties in designing both feedback linearization as well as pure backstepping based strategies. The nonlinear, coupled and switched nature of the wheel slip dynamics leads to further challenges in control design. The key contribution of this paper is the design of a nonlinear hierarchical controller to address the trajectory tracking problem for an autonomous vehicle, in presence of longitudinal as well as lateral slip dynamics, followed by a rigorous Lyapunov based stability analysis.

2. DYNAMIC MODEL OF VEHICLE

2.1 Vehicle Body Model

A rear wheel drive electric vehicle is considered in this study and the dynamics of the vehicle are modeled using the 'bicycle model' (Margolis and Asgari (1991)) given by

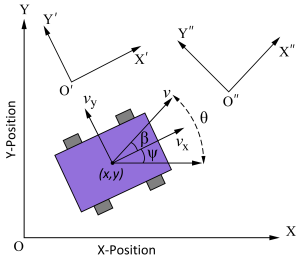

Fig. 1. Vehicle Model in Inertial and Non-Inertial Frames

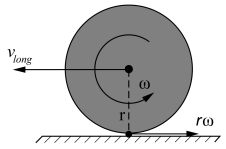

Fig. 2. Tyre Model for Longitudinal Slip

$$m\dot{v_x} = mv_y\dot{\psi} + \Sigma F_x \tag{1}$$

$$m\dot{v_y} = -mv_x\dot{\psi} + \Sigma F_y \tag{2}$$

$$I\ddot{\psi} = \Sigma M \tag{3}$$

where v_x,v_y are the vehicle linear velocities and ΣF_x and ΣF_y are the net forces along x and y directions, respectively, ΣM is the net moment about the vertical axis, m is the mass of the vehicle and I is its moment of inertia about the vertical axis, and $\dot{\psi}$ is the yaw rate. The sideslip angle β represents the direction of resultant velocity of the vehicle and is defined as

$$\beta = tan^{-1}\frac{v_y}{v_x} \tag{4}$$

The resultant velocity of the vehicle is given by

$$v = ||\mathbf{v}|| = \sqrt{{v_x}^2 + {v_y}^2} \tag{5}$$

Fig. 1 shows the vehicle model in inertial $(X-Y)$ and non-inertial $(X'-Y'$, $X''-Y'')$ frames. The resultant velocity $\mathbf{v}$ makes an angle $\theta = \beta + \psi$ with the the X-axis of the inertial frame. The velocity in inertial $(X-Y)$ frame is given by

$$\begin{bmatrix}\dot{x}\\ \dot{y}\end{bmatrix} = v\begin{bmatrix}\cos\theta\\ \sin\theta\end{bmatrix} \tag{6}$$

where (x, y) is the position of centre of mass of the vehicle.

2.2 Tyre Model

For a tyre of radius r, rotating with angular velocity ω and moving with velocity v_{long} as shown in Fig. 2, the slip ratio λ is defined as (Rajamani (2011))

$$\lambda = \begin{cases}\dfrac{r\omega - v_{long}}{r\omega} & r\omega \geq v_{long}\,\text{and}\,\omega, v_{long} \neq 0\\ \dfrac{r\omega - v_{long}}{v_{long}} & r\omega < v_{long}\,\text{and}\,\omega, v_{long} \neq 0\end{cases} \tag{7}$$

Considering the wheel coordinate axes $(X_{wheel} - Y_{wheel})$ as shown in Fig. 3, the force exerted by the wheel may be represented as $\mathbf{F_{wheel}} = [F_{long}\ F_{lat}]^T$ and the wheel velocity may be represented as $\mathbf{v_{wheel}} = [v_{long}\ v_{lat}]^T$, where v_{long} and v_{lat} denote the longitudinal and lateral components of the wheel's velocity. For the rear tyre, $v_{long} = v_x$, since the rear tyre always remains aligned with the longitudinal axis of the vehicle.

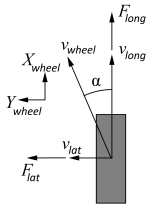

Fig. 3. Tyre's Force, Velocity and Slip Angle α

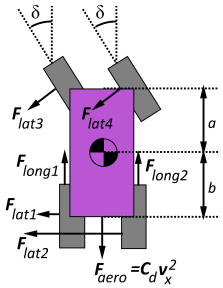

Fig. 4. Free Body Diagram of Vehicle

The force exerted by the tyre, F_{wheel}, is given by Pacejka's tyre model (Bakker et al. (1987); Rajamani (2011); Falcone et al. (2007)). For the sake of simplicity, it is desirable to restrict the slip ratio in the region $|\lambda| \leq \bar{\lambda}$, where the longitudinal force-slip ratio relationship is almost linear, so the longitudinal force may be expressed as (Rajamani (2011))

$$F_{long} = C_x\lambda \tag{8}$$

where C_x is called the longitudinal stiffness of the tyre. Similarly, the lateral or cornering force exerted by the tyre depends on a quantity called 'slip angle'. The slip angle α, as shown in Fig. 3, is defined as Rajamani (2011)

$$\alpha = tan^{-1}\frac{v_{lat}}{v_{long}} \tag{9}$$

For $|\alpha| \leq \bar{\alpha}$, the lateral force-slip angle relationship is almost linear. In this case, the lateral force may be expressed as Rajamani (2011)

$$F_{lat} = -C_y\alpha \tag{10}$$

2.3 Vehicle Dynamics

A free body diagram of the vehicle is illustrated in Fig. 4, where $F_{aero} = C_d{v_x}^2$ is the aerodynamic drag force, F_{long1},F_{long2} are the longitudinal forces exerted by the two rear tyres and F_{lat1}, F_{lat2}, F_{lat3}, F_{lat4} are the lateral forces exerted by the corresponding tyres shown in the figure. The longitudinal and lateral forces exerted by each tyre may be found using (8) and (10). Since the vehicle is a rear-wheel drive, only the rear wheel's longitudinal forces are considered in Fig. 4. Considering the bicycle model, the slip angle for each rear wheel is : $\alpha_3, \alpha_4 = -(\frac{v_y - b\dot{\psi}}{v_x})$, and for each front wheel is : $\alpha_1, \alpha_2 = \delta - (\frac{v_y + a\dot{\psi}}{v_x})$. The lateral force exerted at each wheel (F_{lat1}, F_{lat2}, F_{lat3}, F_{lat4}) may be evaluated by substituting the corresponding wheel's slip angle in (10).

Combining the vehicle body model and the tyre model, assuming small value of steering angle (δ), evaluating slip ratio and slip angle at each wheel and finding the

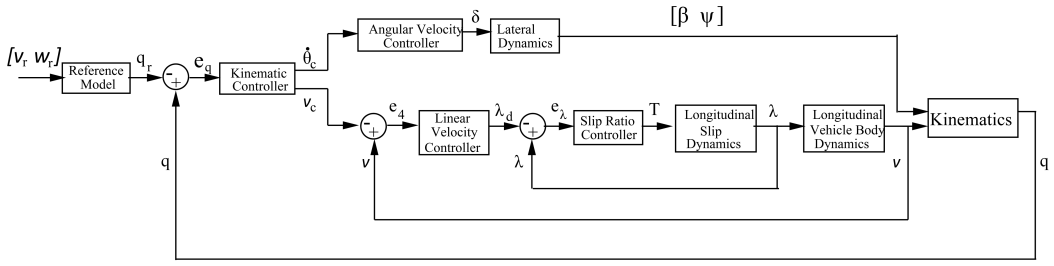

Fig. 5. Block diagram of the proposed nonlinear hierarchical trajectory tracking control system

corresponding tyre forces, the equations of motion for the autonomous vehicle are obtained as

$$\dot{v_x} = v_y\dot{\psi} - C_d {v_x}^2 + \frac{2C_x}{m}\lambda \tag{11}$$

$$\dot{v_y} = -v_x\dot{\psi} + \frac{2(b-a)C_y}{m}\frac{\dot{\psi}}{v_x} - \frac{4C_y}{m}\beta + \frac{2C_y}{m}\delta \tag{12}$$

$$\ddot{\psi} = \frac{2C_y a}{I}\delta + \frac{2C_y(b-a)}{I}\beta - \frac{2C_y(a^2+b^2)}{I}\frac{\dot{\psi}}{v_x} \tag{13}$$

$$\dot{\omega} = \frac{1}{J}(T - rC_x\lambda) \tag{14}$$

where C_d is the coefficient of aerodynamic drag, δ is the steering angle input, T is the torque input to each wheel, J is the moment of inertia of the wheel.

Differentiating (4) with respect to time yields

$$\dot{\beta} = \frac{v_x\dot{v_y} - v_y\dot{v_x}}{v_x^2 + v_y^2} \tag{15}$$

Differentiating (7) with respect to time and substituting (11) and (14) yields

$$\dot{\lambda} = \begin{cases} -\frac{1}{v_x}\Big[(1-\lambda)(v_y\dot{\psi} - \frac{C_d}{m}v_x^2 + \frac{2C_x}{m}\lambda) \\ +\frac{C_x r^2}{J}\lambda(1-\lambda)^2\Big] + \frac{r}{Jv_x}(1-\lambda)^2 T \quad \lambda \geq 0 \\ -\frac{1}{v_x}\Big[(1+\lambda)(v_y\dot{\psi} - \frac{C_d}{m}v_x^2 + \frac{2C_x}{m}\lambda) \\ +\frac{C_x r^2}{J}\lambda\Big] + \frac{r}{Jv_x}T \quad \lambda < 0 \end{cases} \tag{16}$$

Although the right hand side of (16) is a switching function, it is still continuous. Equations (11), (12), (13) and (16) comprise the plant dynamics for control design.

Remark 1. The slip ratio dynamics in (16) are jerk-level i.e. one order higher than the acceleration-level dynamics in (11), so it is reasonable to use acceleration $\dot{v_x}$ as feedback for the control design.

Assumption 1. $v_x \geq v_{min} > 0$. This also implies from (4) that $\beta \neq \frac{\pi}{2}$.

Assumption 2. Slip ratio $|\lambda| \leq \bar{\lambda}$ and slip angle $|\alpha| \leq \bar{\alpha}$, so that the longitudinal force-slip ratio and lateral force-slip angle relationship are linear.

Assumption 1 is required for controllability of the system. A similar condition is also encountered in (Oriolo et al. (2002)), where a singularity may arise in the controller, when a wheeled mobile robot attains zero velocity. Assumption 2 implies that (8) and (10) hold.

3. CONTROL DESIGN

3.1 Objective

For the given reference model :

$$\dot{x_r} = v_r\cos\theta_r \tag{17}$$

$$\dot{y_r} = v_r\sin\theta_r \tag{18}$$

$$\dot{\theta_r} = w_r \tag{19}$$

with $v_r(t) \geq v_{min} > 0$ for all time t, the objective is for $\mathbf{q} = [x\, y\, \theta]^T$ to track $\mathbf{q_r} = [x_r\, y_r\, \theta_r]^T$.

Assumption 3. Reference speed $v_r(t)$ and reference yaw rate $w_r(t)$ are bounded.

3.2 Hierarchical Control Design Procedure

A nonlinear hierarchical controller is proposed as illustrated in Fig. 5; the outer loop kinematic controller assigns a desired linear velocity v_c and angular velocity $\dot{\theta}_c$ based on position error feedback, which are then fed into the lateral and longitudinal subsystems. The lateral subsystem involves an angular velocity controller, which assigns the steering angle input δ, while the longitudinal subsystem involves a cascade with two loops. The outer loop linear velocity controller of the longitudinal subsystem assigns the desired slip ratio λ_d, which is then used by the inner loop slip ratio controller to generate the torque input T.

The tracking error in vehicle frame is given by

$$\mathbf{e_q} = R(\mathbf{q_r} - \mathbf{q}) = \begin{bmatrix} e_1 \\ e_2 \\ e_3 \end{bmatrix} = \begin{bmatrix} \cos\theta & \sin\theta & 0 \\ -\sin\theta & \cos\theta & 0 \\ 0 & 0 & 1 \end{bmatrix} \begin{bmatrix} x_r - x \\ y_r - y \\ \theta_r - \theta \end{bmatrix} \tag{20}$$

where $e_3 \in [-\pi, \pi]$, since it is the orientation error. Then the orientation tracking problem may also be expressed as the problem of regulating $\sin(\frac{e_3}{2})$ to 0. In order to find the kinematics, differentiating (20) with respect to time yields

$$\dot{\mathbf{e_q}} = \begin{bmatrix} \dot{\theta}e_2 + v_r\cos e_3 \\ -\dot{\theta}e_1 + v_r\sin e_3 \\ w_r \end{bmatrix} - \begin{bmatrix} 1 & 0 \\ 0 & 0 \\ 0 & 1 \end{bmatrix} \begin{bmatrix} v \\ \dot{\theta} \end{bmatrix} \tag{21}$$

Step 1 : Auxilliary Velocity (Kinematic) Control Inputs

The auxilliary velocity inputs stabilising (21) are defined as Kanayama et al. (1990)

$$\begin{bmatrix} v_c \\ \dot{\theta}_c \end{bmatrix} \triangleq \begin{bmatrix} v_r \cos e_3 + k_1 e_1 \\ w_r + k_2 v_r e_2 + k_3 \sin e_3 \end{bmatrix} \tag{22}$$

with $k_1, k_2, k_3 > 0$. The error e_4 for the virtual linear velocity control is defined as

$$e_4 \triangleq v - v_c \tag{23}$$

After substituting (22) and (23) in (21), the following expression for $\dot{\mathbf{e_q}}$ is obtained

$$\dot{\mathbf{e_q}} = \begin{bmatrix} \dot{\theta} e_2 - k_1 e_1 - e_4 \\ -\dot{\theta} e_1 + v_r \sin e_3 \\ -k_2 v_r e_2 - k_3 \sin e_3 \end{bmatrix} \tag{24}$$

Considering the following Lyapunov function candidate

$$V_1 = k_1(e_1^2 + e_2^2) + 2\frac{k_1}{k_2}(1 - \cos e_3) \tag{25}$$

The time derivative of V_1 after substituting (24) is found to be

$$\dot{V_1} = -2k_1^2 e_1^2 - 2\frac{k_1 k_3}{k_2}\sin^2 e_3 - 2k_1 e_1 e_4 \tag{26}$$

A virtual control for $\dot{\theta}_c$ was not considered here because it is possible to perfectly track $\dot{\theta}_c$, which gets clear in the subsequent analysis. For this purpose, an error variable $e_{\dot{\theta}}$ is introduced for $\dot{\theta}_c$,

$$e_{\dot{\theta}} = \dot{\theta} - \dot{\theta}_c \tag{27}$$

Since the right hand side of (27) contains $\dot{\theta}$, an expression for $\dot{\theta}$ is obtained by differentiating $\theta = \beta + \psi$ with respect to time and substituting (15),

$$\dot{\theta} = \dot{\beta} + \dot{\psi} = \frac{v_x \dot{v_y} - v_y \dot{v_x}}{v_x^2 + v_y^2} + \dot{\psi} \tag{28}$$

since the right hand side of (28) contains $\dot{v_y}$, which is related to the steering angle control input δ in (12). At this stage, δ is designed as

$$\delta = \frac{m}{2C_y}(u_{ay} + v_x \dot{\psi}) - (b-a)\frac{\dot{\psi}}{v_x} + 2\beta \tag{29}$$

where u_{ay} is a control term yet to be designed. Substituting (29) in (12) yields

$$\dot{v_y} = u_{ay} \tag{30}$$

Since it is desirable to design u_{ay} such that the remaining terms get cancelled in (28), u_{ay} is designed as

$$u_{ay} = \frac{v_y \dot{v_x}}{v_x} + \frac{v_x^2 + v_y^2}{v_x} u_\beta \tag{31}$$

where u_β is a control term yet to be designed. Substituting (31) in (15) yields

$$\dot{\beta} = u_\beta \tag{32}$$

Designing u_β as

$$u_\beta = -\dot{\psi} + \dot{\theta_c} \tag{33}$$

yields $\dot{\theta} = \dot{\theta_c}$, and therefore $e_{\dot{\theta}} = 0$.

Step 2 : Regulating e_4

The time derivative of e_4 from (23), is

$$\dot{e_4} = \dot{v} - \dot{v_c} = a_r + e_5 - \dot{v_c} \tag{34}$$

where a_r is the virtual control for acceleration and e_5 is the corresponding backstepping error, defined as

$$e_5 \triangleq \dot{v} - a_r \tag{35}$$

The virtual control for $\dot{v}$, stabilizing (34) in subsequent analysis, is

$$a_r = \dot{v_c} - k_4 e_4 + 2k_1 k_4 e_1 \tag{36}$$

with $k_4 > 0$, where $\dot{v_c}$ is obtained after differentiating (22) with respect to time.

$$\dot{v_c} = \dot{v_r}\cos e_3 - v_r \dot{e_3}\sin e_3 + k_1 \dot{e_1} \tag{37}$$

At this stage, consider the following Lyapunov function candidate

$$V_2 = V_1 + \frac{1}{2k_4}e_4^2 \tag{38}$$

The time derivative of V_2 after substituting (36), (37) and (35) is expressed as

$$\dot{V_2} = -2k_1^2 e_1^2 - 2\frac{k_1 k_3}{k_2}\sin^2 e_3 - e_4^2 + \frac{1}{k_4} e_4 e_5 \tag{39}$$

Step 3: Regulating e_5

Since e_5 involves $\dot{v}$ in (35), it is required to find $\dot{v}$, so (5) is differentiated with respect to time and (4) is substituted in the resultant expression. Then

$$\dot{v} = \dot{v_x}\cos\beta + \dot{v_y}\sin\beta \tag{40}$$

Substituting (11) in (40) yields

$$\begin{aligned} \dot{v} &= (v_y\dot{\psi} - C_d {v_x}^2 + \frac{2C_x}{m}\lambda)\cos\beta + \dot{v_y}\sin\beta \\ &= (v_y\dot{\psi} - C_d {v_x}^2 + \frac{2C_x}{m}(u_\lambda + e_\lambda))\cos\beta + \dot{v_y}\sin\beta \end{aligned} \tag{41}$$

where u_λ is the virtual control for λ and e_λ is the corresponding backstepping error, defined as

$$e_\lambda = \lambda - u_\lambda \tag{42}$$

At this stage, u_λ is designed as

$$u_\lambda = \frac{m}{2C_x}(C_d v_x^2 - v_y\dot{\psi} + \frac{1}{\cos\beta}(-\dot{v_y}\sin\beta + a_r)) \tag{43}$$

Substituting (43) in (41), and the resultant expression in (35) yields

$$e_5 = \frac{2C_x}{m} e_\lambda \cos\beta \tag{44}$$

The time derivative of e_5, obtained after differentiating (44) with respect to time is

$$\dot{e_5} = \frac{2C_x}{m}\dot{e_\lambda}\cos\beta - \frac{2C_x}{m}e_\lambda\dot{\beta}\sin\beta \tag{45}$$

In order to find $\dot{e_\lambda}$, (42) is differentiated with respect to time.

$$\dot{e_\lambda} = \dot{\lambda} - \dot{u_\lambda} \tag{46}$$

Since (46) contains $\dot{\lambda}$ on the right hand side, it may be recalled from (16), that $\dot{\lambda}$ depends on the wheel torque T, which is the actual control term. Since (16) consists of a switching function, the wheel torque input T is also designed appropriately as a switching function, to cancel the switching terms.

$$T = \begin{cases} \frac{Jv_x}{r(1-\lambda)^2}\Big[u_{\dot\lambda} + \frac{1}{v_x}\big((1-\lambda)(v_y\dot\psi \\ -\frac{C_d}{m}v_x^2 + \frac{2C_x}{m}\lambda) + \frac{C_x r^2}{J}\lambda(1-\lambda)^2\big)\Big] & \lambda \geq 0 \\ \frac{Jv_x}{r}\Big[u_{\dot\lambda} + \frac{1}{v_x}\big((1+\lambda)(v_y\dot\psi \\ -\frac{C_d}{m}v_x^2 + \frac{2C_x}{m}\lambda) + \frac{C_x r^2}{J}\lambda\big)\Big] & \lambda < 0 \end{cases} \tag{47}$$

where $u_{\dot\lambda}$ is a control term yet to be designed. It may be observed that the expression for T in (47) is continuous, if $u_{\dot\lambda}$ is continuous. In order to find the closed loop dynamics, substituting (47) in (16) yields

$$\dot\lambda = u_{\dot\lambda} \tag{48}$$

The closed loop dynamics in (48) does not involve any switching term. Substituting (48) in (46), and the resultant expression along with (32) in (45) gives

$$\dot e_5 = \frac{2C_x}{m}(u_{\dot\lambda} - \dot u_\lambda)\cos\beta - \frac{2C_x}{m}e_\lambda u_\beta \sin\beta \tag{49}$$

At this stage, $u_{\dot\lambda}$ is designed as

$$u_{\dot\lambda} = \dot u_\lambda + e_\lambda u_\beta \tan\beta - k_5 e_5 - \frac{m}{2C_x\cos\beta}e_4 \tag{50}$$

where $k_5 > 0$. Since the right hand side in (50) contains $\dot u_\lambda$, an expression for $\dot u_\lambda$ needs to be found. Substituting (36) in (43) gives

$$u_\lambda = \frac{m}{2C_x}(C_d v_x^2 - v_y\dot\psi + \frac{1}{\cos\beta}(\dot v_c - k_4 e_4 + 2k_1 k_4 e_1)) \tag{51}$$

Differentiating (51) with respect to time, and substituting (32), yields

$$\begin{aligned} \dot u_\lambda = \frac{m}{2C_x}\Big[2C_d v_x \dot v_x - \dot v_y\dot\psi \\ + \frac{1}{\cos^2\beta}\Big((\ddot v_c - k_4\dot e_4 + 2k_1k_4\dot e_1)\cos\beta \\ -(\dot v_c - k_4 e_4 + 2k_1k_4 e_1)u_\beta\sin\beta\Big)\Big] \end{aligned} \tag{52}$$

The right hand side of (52) contains $\ddot v_c$, which is obtained by differentiating (37) with respect to time

$$\ddot v_c = \ddot v_r\cos e_3 - 2\dot v_r\dot e_3\sin e_3 - v_r\ddot e_3 + k_1\dot e_1 - v_r\dot e_3{}^2\cos e_3 + k_1\ddot e_1 \tag{53}$$

Substituting (37) and (53) in (52) gives

$$\begin{aligned} \dot u_\lambda = \frac{m}{2C_x}\Big[2C_d v_x\dot v_x - \dot v_y\dot\psi + \frac{1}{\cos^2\beta}\Big((\ddot v_r\cos e_3 \\ -2\dot v_r\dot e_3\sin e_3 - v_r\ddot e_3 + k_1\dot e_1 - v_r\dot e_3{}^2\cos e_3 + k_1\ddot e_1 \\ -k_4\dot e_4 + 2k_1k_4\dot e_1)\cos\beta - (\dot v_r\cos e_3 - v_r\dot e_3\sin e_3 \\ +k_1\dot e_1 - k_4 e_4 + 2k_1k_4 e_1)u_\beta\sin\beta\Big)\Big] \end{aligned} \tag{54}$$

where the expressions for $\ddot e_1$ and $\ddot e_3$ are obtained after differentiating (24) as follows

$$\begin{aligned} \ddot e_1 = (\dot w_r + k_2\dot v_r e_2 + k_2 v_r\dot e_2 + k_3\dot e_3\cos e_3)e_2 + \\ (w_r + k_2 v_r e_2 + k_3\sin e_3)\dot e_2 - k_1\dot e_1 - \dot e_4 \end{aligned} \tag{55}$$

$$\ddot e_3 = -k_2\dot v_r e_2 - k_2 v_r\dot e_2 - k_3\dot e_3\cos e_3 \tag{56}$$

These expressions along with (24) can be back-substituted into (54), and the required control input T may be obtained after further back-substituting $\dot u_\lambda$ in (54) and then back-subsituting the resultant expression for $u_{\dot\lambda}$ into (47).

For analysing stability of the closed loop system, the expression for $\dot e_5$, found after substituting (50) in (49), is

$$\dot e_5 = -\frac{2C_x}{m}k_5 e_5\cos\beta - e_4 \tag{57}$$

At this stage, consider the following Lyapunov function candidate

$$V_3 = V_2 + \frac{1}{2k_4}e_5^2 \tag{58}$$

The expression for time derivative of V_3, obtained after differentiating (58) is

$$\dot V_3 = \dot V_2 - \frac{2C_x}{mk_4}k_5 e_5^2\cos\beta - \frac{e_4 e_5}{k_4} \tag{59}$$

Substituting the expression for $\dot V_2$ from (39) into (59),

$$\dot V_3 = -2k_1^2 e_1^2 - 2\frac{k_1k_3}{k_2}\sin^2 e_3 - e_4^2 - \frac{2C_x}{mk_4}k_5 e_5^2\cos\beta \tag{60}$$

It may be recalled at this stage, that $\cos\beta > 0$, since $\beta \in (-\pi/2, \pi/2)$. From (60), $\dot V_3$ is negative semi-definite, implying that the error vector $\mathbf{e} = [e_1\ e_2\ e_3\ e_4\ e_5]^T$ is bounded. Since $\mathbf{e}$ is bounded, it may be observed from (24), (34), (37) and (57) that $||\mathbf{e}||$ and $||\dot{\mathbf{e}}|| \in \mathcal{L}_\infty$, so $\ddot V_3 \in \mathcal{L}_\infty$. Hence $\dot V_3$ is uniformly continuous, and since V_3 is lower bounded and $\dot V_3$ is negative semi-definite, by Barbalat's lemma, it follows that $\dot V_3 \to 0$. Thus from the right hand side of (60), it follows that $[e_1\ e_3\ e_4\ e_5]^T \to 0$.

The orientation error derivative $\dot e_3$ is uniformly continuous as $\ddot e_3 = -k_2\dot v_r e_2 - k_2 v_r\dot e_2 - k_3\dot e_3\cos e_3 \in \mathcal{L}_\infty$, because of the fact that $||\mathbf{e}||$ and $||\dot{\mathbf{e}}|| \in \mathcal{L}_\infty$, and $v_r \in \mathcal{L}_\infty$ according to Assumption 4. Using Barbalat's lemma, it follows that $\dot e_3 \to 0$. This implies with the use of (24) that $\dot e_3 = -k_2 v_r e_2 - k_3\sin e_3 \to 0$. Since $e_3 \to 0$ and $v_r > 0$, it follows that $e_2 \to 0$. Thus $e = [e_1\ e_2\ e_3\ e_4\ e_5]^T \to 0$.

4. SIMULATION RESULTS

The control design procedure explained in Section III was implemented in Simulink. The simulation considered a Formula Style Rear-Wheel Drive Electric Car, used for Formula Student competitions. The vehicle parameters were considered as : $m = 280, I = 85, C_d = 0.8, a = 1.2, b = 0.8, C_x = 30000, C_y = 20000, r = 0.235, J = 0.4$ The following controller parameters were used in the simulation : $k_1 = 50, k_2 = 2, k_3 = 30, k_4 = 10, k_5 = 0.5$. A hyperbolic tangent shaped lane change reference trajectory was considered for the simulation.

Fig. 6 (a) shows the actual and desired trajectories, 6 (b) the longitudinal tracking error, 6 (c) the lateral tracking error, 6 (d) the angular error, 6 (e) the torque input and 6 (f) the steering angle input. It is evident from the simulation results, that the reference trajectory is tracked and all the tracking and backstepping errors converge to zero.

5. CONCLUSION

A nonlinear hierarchical trajectory tracking controller is proposed, for an autonomous ground vehicle with combined longitudinal and lateral wheel-slip dynamics. The stability of the closed-loop system is guaranteed using Lyapunov analysis, and simulation results are provided to demonstrate the efficacy of the controller. In this paper, it

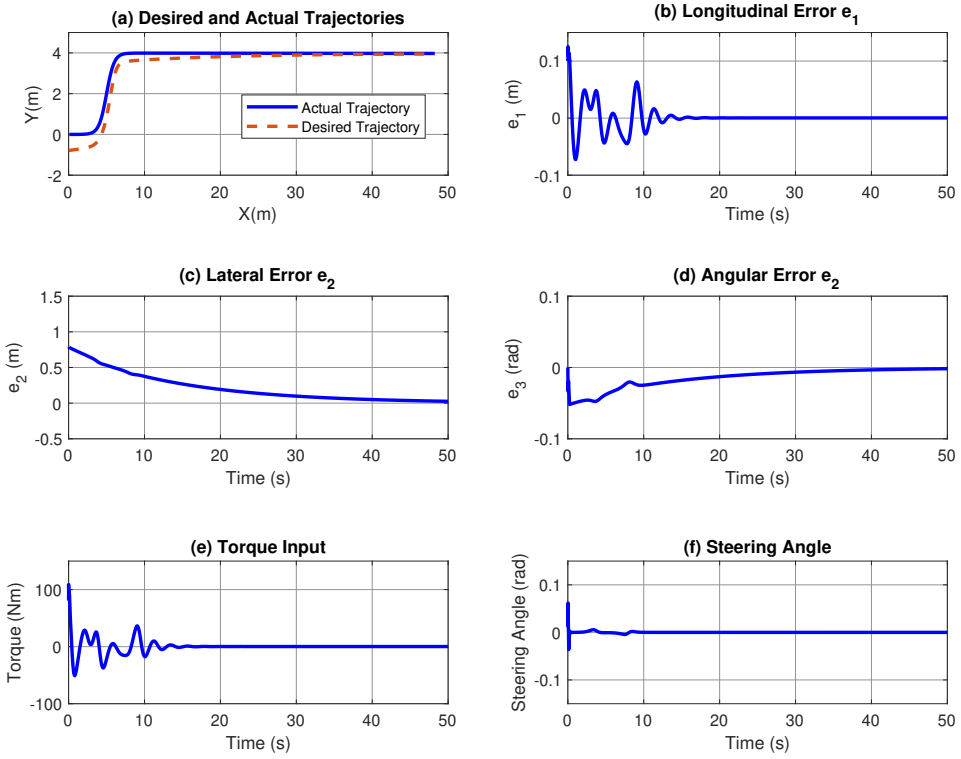

Fig. 6. (a)Desired and Actual Trajectories, (b) Longitudinal Tracking Error, (c) Lateral Tracking Error, (d) Angular Tracking Error, (e) Torque Input and (f) Steering Input from the simulation result

is assumed that slip ratios and slip angles lie in a bounded region such that they have a linear relationship with the traction forces. It is also assumed that the longitudinal velocity is greater than some positive constant, in order to avoid singularity. The future goal of this work is to design a controller, such that the longitudinal velocity remains constrained to be greater than some positive constant, the slip ratios and the slip angles are kept bounded in the desired region, and the controller is robust to parametric uncertainty.

REFERENCES

Aguiar, A.P. and Hespanha, J.P. (2007). Trajectory-tracking and path-following of underactuated autonomous vehicles with parametric modeling uncertainty. *IEEE Transactions on Automatic Control*, 52(8), 1362–1379.

Bakker, E., Nyborg, L., and Pacejka, H.B. (1987). Tyre modelling for use in vehicle dynamics studies. Technical report, SAE Technical Paper.

Chen, C., Jia, Y., Shu, M., and Wang, Y. (2015). Hierarchical adaptive path-tracking control for autonomous vehicles. *IEEE Transactions on Intelligent Transportation Systems*, 16(5), 2900–2912.

Falcone, P., Borrelli, F., Asgari, J., Tseng, H.E., and Hrovat, D. (2007). Predictive active steering control for autonomous vehicle systems. *IEEE Transactions on control systems technology*, 15(3), 566–580.

Jiang, J. and Astolfi, A. (2018). Lateral control of an autonomous vehicle. *IEEE Transactions on Intelligent Vehicles*, 3(2), 228–237.

Kanayama, Y., Kimura, Y., Miyazaki, F., and Noguchi, T. (1990). A stable tracking control method for an autonomous mobile robot. In *Proceedings., IEEE International Conference on Robotics and Automation*, 384–389. IEEE.

Margolis, D.L. and Asgari, J. (1991). Multipurpose models of vehicle dynamics for controller design. Technical report, SAE Technical Paper.

Oriolo, G., De Luca, A., and Vendittelli, M. (2002). Wmr control via dynamic feedback linearization: design, implementation, and experimental validation. *IEEE Transactions on control systems technology*, 10(6), 835–852.

Quirynen, R., Berntorp, K., and Di Cairano, S. (2018). Embedded optimization algorithms for steering in autonomous vehicles based on nonlinear model predictive control. In *2018 Annual American Control Conference (ACC)*, 3251–3256. IEEE.

Rajamani, R. (2011). *Vehicle dynamics and control*. Springer Science & Business Media.